THE JOURNAL OF PHYSICAL CHEMISTRY C

Article

pubs.acs.org/JPCC

Unusual Pressure Effect on the Shear Modulus in $MgAl_2O_4$ Spinel

Yongtao Zou,[†,‡,*] Steeve Gréaux,[†] Tetsuo Irifune,[†] Baosheng Li,[‡] and Yuji Higo[§]

[†]Geodynamics Research Center, Ehime University, Matsuyama 790-8577, Japan

[‡]Mineral Physics Institute, State University of New York, Stony Brook, New York 11794, United States

[§]Japan Synchrotron Radiation Institute, Hyogo 679-5198, Japan

ABSTRACT: Compressional (V_P) and shear (V_S) wave velocities of polycrystalline $MgAl_2O_4$ spinel have been measured up to 14 GPa and 900 K using ultrasonic interferometry and in situ X-ray diffraction techniques. Here, we observed a weaker pressure dependence in shear modulus (G) for $MgAl_2O_4$ spinel, as compared to a stronger $\partial G/\partial P$ for magnesium silicate/germanate counterpart. Our first-principles calculations show that the tetragonal shear modulus $C_S = (C_{11}-C_{12})/2$ decrease with pressures, indicating acoustic mode softening, which further supports our observed experimental results. Using a finite strain equation of state approach the elastic bulk and shear moduli, as well as their pressure and temperature derivatives, are derived from the directly measured velocities and densities, yielding K_{S0} =196.0(9) GPa, G_0 = 109.0(4) GPa, $\partial K_S/\partial P$ = 4.60(9), and $\partial G/\partial P$ = 0.58(3) independent of pressure calibration. The temperature derivatives for the bulk and shear moduli were tightly constrained from acoustic velocity measurements as $\partial K_S/\partial T = -0.022(3)$ GPa/K and $\partial G/\partial T = -0.014(1)$ GPa/K. In addition, the mechanism for the unusual pressure effect on the shear modulus in $MgAl_2O_4$ spinel has been addressed by the coupling between atomic displacements and shear strains, namely a better accommodation of the AlO_6 octahedral distortion and shear strains, as well as the pressure-induced tilting/distortion and/or symmetry changes in $MgAl_2O_4$ spinel.

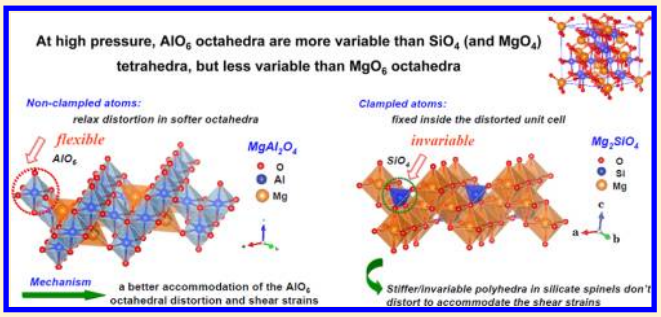

I. INTRODUCTION

Magnesium aluminate ($MgAl_2O_4$) spinel is considered as an important material, widely used in both civil and military industrials as electrical dielectric and window material, as well as a covering material in high-pressure discharge lamps,[1−4] because of its attractive combination of the properties of high melting point, good mechanical strength, high resistance against chemical attack, and good optical properties.[5−8] Moreover, $MgAl_2O_4$ spinel also plays a significant role in geophysics as an important rock-forming mineral, which constitutes peridotites from the uppermost of the Earth's mantle.[9,10] Therefore, understanding the elastic behavior of $MgAl_2O_4$ spinel is of great importance in the fields ranging from materials science to geophysics.

Elastic properties of $MgAl_2O_4$ spinel for both single crystal and synthetic polycrystalline samples have been investigated by experimental studies using ultrasonic measurements,[11−14] Brillouin scattering spectroscopy,[15] resonant sphere technique,[16] and static compression experiments,[17,18] as well as theoretical calculations using first-principles.[19,20,22] An earlier experimental study on the acoustic velocities of $MgAl_2O_4$ spinel was conducted by Chang and Barsch[14] to 1 GPa, predicting shear modulus softening at an extrapolated pressure of ∼10 GPa. Subsequently, Yoneda[13] performed ultrasonic elastic wave velocity measurements on $MgAl_2O_4$ spinel in a multianvil apparatus to ∼6.2 GPa at room temperature, where a negative pressure derivative for the shear wave velocity in {110} crystal plane was observed and the shear modulus was found to increase slightly with pressures but with a larger uncertainty ($\partial G/\partial P$ = 0.4(5)). Recently, a fluorescence sideband measurement of polycrystalline $MgAl_2O_4$ spinel by Chopelas[23] reported an almost invariable shear wave velocity with increasing pressures up to 11 GPa at room temperature in a diamond anvil cell, resulting in an even lower value of $\partial G/\partial P$ = 0.07, which strongly depended on the vibrational mode.[23] For $MgSiO_3$ orthopyroxene, anomalous elastic behavior (elastic softening) was observed by Kung et al.[24] using ultrasonic interferometry and in situ X-radiation techniques, which is suggested to be associated with a transition to a metastable phase intermediate between orthorhombic enstatite and high-pressure clino-enstatite. Elasticity of single-crystal $MgAl_2O_4$ spinel as a function of temperature was investigated to 1273 K at ambient pressure using Brillouin scattering technique by Askarpour et al.[15] From the temperature dependence of acoustic velocities, an order−disorder phase transition was observed at ∼923 K (ref 15). In contrast, this order−disorder phase transition has not been observed by Yeganeh-Haeri et al.[25] using a similar technique for measurements with temperatures up to 973 K.

In view of previous studies,[13,23,26,27] it is interesting to find that the low pressure dependence in shear moduli appear to be common for some nonsilicate/germanate spinels such as

Received: May 18, 2013
Revised: October 28, 2013
Published: October 30, 2013

   dx.doi.org/10.1021/jp404901a | J. Phys. Chem. C 2013, 117, 24518−24526

$(Zn_{0.74}Fe_{0.18}Mg_{0.08})Al_{1.99}O_4$ gahnite[26] ($\partial G/\partial P$ = 0.5) and Fe_3O_4 magnetite[27] ($\partial G/\partial P$ = −0.1), unlike silicate/germanate counterparts. Despite its interest, the elastic bulk and shear properties are still not well studied, and the mechanism and/or atomistic origin for the softening shear properties under pressure are also unknown. In addition, to date no direct measurement (i.e., acoustic measurement) of the elasticity has been conducted at simultaneous high pressure and high temperature. All of the previous studies on the elastic properties/sound velocities of $MgAl_2O_4$ spinel were performed at either high pressure or high temperature.[11−16] For a better understanding of the thermoelasticity of $MgAl_2O_4$ spinel as well as its high-pressure and high-temperature behavior, it is crucial to measure the acoustic velocities at simultaneous high $P-T$ conditions. This simultaneous measurement has become possible using the recent state-of-the-art techniques of ultrasonic interferometry in conjunction with X-ray radiation in a multianvil apparatus.[28−32]

In this paper, simultaneous high-pressure and high-temperature acoustic measurements on polycrystalline $MgAl_2O_4$ spinel have been conducted using ultrasonic interferometry and X-ray diffraction measurements in a multianvil apparatus up to 14 GPa and 900 K. Here, we report a possible mechanism for the unusual pressure effect on the shear modulus in $MgAl_2O_4$ spinel, together with new results of compressional and shear wave velocities as well as thermoelastic properties. The elastic moduli and their pressure and temperature derivatives are precisely determined from the measured velocity and density data using a pressure-standard-free fitting to third-order finite strain equations.[31,32]

II. EXPERIMENTAL SECTION

Synthesis and Characterization of Polycrystalline $MgAl_2O_4$ Spinel. Magnesium aluminate spinel can be described by $[Mg_{(1-x)}Al_x]^{IV}[Mg_xAl_{(2-x)}]^{VI}O_4$, in which normal spinel (inversion parameter x = 0) has all the Mg atoms in tetrahedral sites and Al atoms in octahedral sites; inverse spinel (x = 1) occupies half of the Al and all the Mg atoms in octahedral sites and half of the Al atoms in tetrahedral sites. The polycrystalline $MgAl_2O_4$ spinel sample was hot-pressed from pure $MgAl_2O_4$ powder starting material (Alfa Aesar, claimed 99% purity) at 10 GPa and 1000 °C in a Kawai-type multianvil apparatus at Geodynamics Research Center, Ehime University, Japan. The $MgAl_2O_4$ powder was dried in an oven and then enclosed in a gold capsule with a wall thickness of 0.1 mm. Tungsten carbide cubic anvils with 8 mm truncation edge length were used as the second stage anvils of the high-pressure apparatus. The pressure medium was a semisintered (Mg,Co)O octahedron of 11 mm in edge length into which a cylindrical $LaCrO_3$ heater was inserted. In this hot-pressing experiment, a special $P-T$ path[29] was designed to relax intergranular stress for obtaining a well-sintered sample. According to the previous studies on the pressure and temperature dependences of cation disorder in $MgAl_2O_4$ spinel,[33−35] we estimate the inversion parameter for the synthesized polycrystalline spinel at 10 GPa and 1000 °C to be x = 0.24 (i.e., $[Mg_{0.76}Al_{0.24}][Mg_{0.24}Al_{0.76}]O_4$). The synthesized sample with ∼2 mm in diameter and ∼1.5 mm in length appeared to be translucent, well-sintered and free of visible macro-cracks. X-ray diffraction (XRD) pattern showed that the synthetic specimen was a single phase of $MgAl_2O_4$ spinel, as shown in Figure 1. SEM observations before our measurements (Figure 2a) revealed that the synthetic sample was free of visible microcracks with an

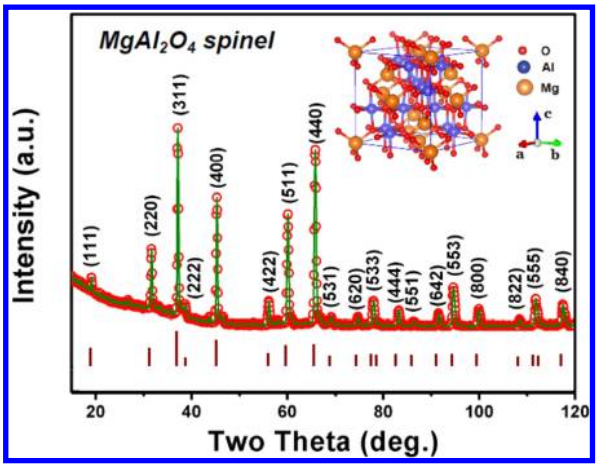

Figure 1. X-ray diffraction pattern of the synthesized $MgAl_2O_4$ specimen for the present ultrasonic measurements, showing that the sample was a single phase of spinel structured material, and no secondary phase such as corundum (Al_2O_3) and/or periclase (MgO) observed within the resolution of the current X-ray diffraction.

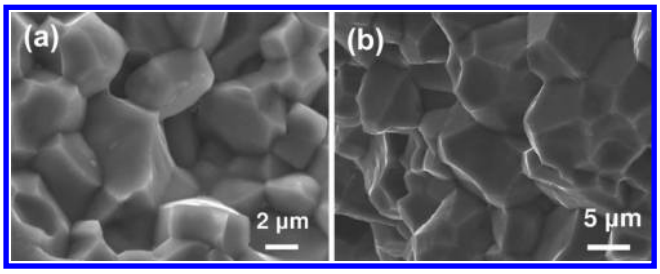

Figure 2. (a). SEM image showing the microstructure of the synthetic polycrystalline $MgAl_2O_4$ spinel used for the present sound velocity measurements. The average grain size of the synthetic sample observed from SEM is about 4−5 μm; (b) SEM image of the recovered sample after ultrasonic measurement, showing that the specimen is still pure $MgAl_2O_4$ spinel structure and its homogeneous fine grains.

average grain size of about 4−5 μm. As measured by Archimedes immersion method, the bulk density of the sample was determined to be 3.57(2) g/cm^3 with a porosity of ∼0.5%. Figure 2b is an SEM image of the recovered sample after our ultrasonic measurements, showing that there is no significant grain growth in our $MgAl_2O_4$ specimen during our experiments, and the specimen exhibits an equilibrated microstructure with homogeneous fine grains.

Ultrasonic Elastic Wave Velocity Measurements of $MgAl_2O_4$ Spinel at Simultaneous High $P-T$ Conditions. Compressional (P) and shear (S) wave velocities of polycrystalline $MgAl_2O_4$ spinel at high pressure and high temperature were measured using ultrasonic interferometry technique combined with in situ X-ray radiation and radiography in a multianvil high-pressure apparatus at the beamline BL04B1 of SPring-8, Japan. Details of this experimental setup and the ultrasonic interferometry were described elsewhere.[28−32] Briefly, the pressure-transmitting medium was a semisintered (Mg, Co)O octahedron. $LaCrO_3$ sleeve was used as a thermal insulator, and MgO window was placed in $LaCrO_3$ sleeve for obtaining X-ray diffraction of the specimen. A dual-mode $LiNbO_3$ transducer (10° Y-cut) was mounted with a high-temperature epoxy on a truncated corner of a WC anvil cube, which generates and receives both P and S signals simultaneously. At high pressures, the transducer remains free

dx.doi.org/10.1021/jp404901a | J. Phys. Chem. C 2013, 117, 24518−24526

of stress, because it is located in the gap between the first-stage anvils and the second-stage cubes. To minimize the loss of acoustic energy, all surfaces along the acoustic path, including the ends of the WC cube with transducer mounted, alumina buffer rod, and the specimen, were well polished using 1 μm diamond paste. Inside the cell assembly, the front surface of the sample was in contact with an alumina (Al_2O_3) buffer rod via a gold film (2 μm) to improve their mechanical coupling, whereas the rear surface of the sample was backed by a pressure marker disk (Au + BN) with the same gold film as couplant. Temperature was monitored with a $W_{97}Re_3$–$W_{75}Re_{25}$ thermocouple located at the opposite side of the sample for measuring the temperature.

Travel times for P and S waves were simultaneously measured using the transfer function method[31] with standard deviation of ~0.4 ns for S waves and ~0.2 ns for P waves.[31,32] The sample length at high pressure and high temperature was directly obtained by X-radiographic imaging method; the precision of this direct measurement of sample length was estimated to be 0.2–0.4%.[31,32] During our experiments, X-ray diffraction patterns for both the specimen and pressure marker are collected using a solid-state detector, which is mounted on a stage behind the high-pressure press set at a diffraction angle of $2\theta \approx 6.0°$. The collected X-ray diffraction patterns of the sample are refined to determine the unit-cell volume, from which the densities at high pressures and temperatures are obtained according to the density and unit-cell volume at ambient conditions.

First-Principles Calculations. Our first-principles calculations are performed with the CASTEP code,[36] based on density functional theory (DFT) using Vanderbilt-type ultrasoft pseudopotentials and a plane-wave expansion of the wave functions.[37] The local density approximation (LDA) was employed for determination of the exchange and correlation potentials for electron–electron interactions. The Broyden–Fletcher–Goldfarb–Shanno optimization method was applied to search for the ground states of $MgAl_2O_4$ spinel. For the Brillouin-zone sampling, the Monkhorst–Pack scheme[38] was adopted.

To confirm the convergence of our calculations, we have carefully analyzed the dependences of the total energy on the cutoff energy from 300 to 750 eV and the k-point set mesh according to the Monkhorst–Pack grid. During our first-principles calculations, the difference in total energy is minimized to below 8×10^{-6} eV/atom, the maximum ionic Hellmann–Feynman force is converged to less than 0.01 eV/Å, and the total stress tensor is reduced to the order of 0.02 GPa by using the finite basis-set corrections. The valence configuration is $3s^2 2p^6$, $3s^2 3p^1$, and $2s^2 2p^4$ for Mg, Al, and O, respectively. Integrations in the Brillouin zone are performed using special k-points generated with $5 \times 5 \times 5$. One-electron valence states are expanded on a basis of plane waves with a cutoff energy of 710 eV in the electronic property calculations. All these parameters have been tested to be sufficient for the convergence.

III. RESULTS AND DISCUSSION

In this experiment, we performed five heating/cooling cycles at pressures ranging from 5.4 to 14.4 GPa and temperatures up 900 K. The sample was annealed at the peak temperature of each cycle for several minutes to release nonhydrostatic stress accumulated during cold compression/decompression. After annealing, we collected the data of ultrasonic travel times, sample images, and X-ray diffraction patterns for both the sample and pressure marker at every 200 K during cooling. Representative X-ray diffraction patterns for $MgAl_2O_4$ spinel collected at ambient and high P–T conditions are shown in Figure 3. Energy-dispersive X-ray diffraction patterns obtained

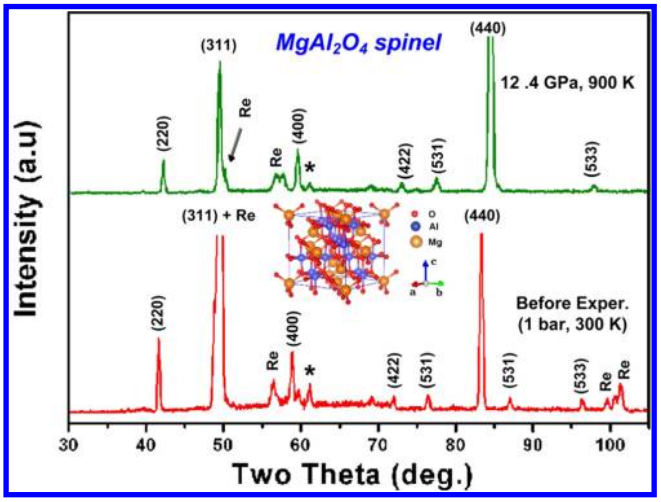

Figure 3. Representative X-ray diffraction patterns for $MgAl_2O_4$ spinel collected at ambient and high P–T conditions, showing that the specimen remains in pure spinel phase without secondary phases, such as corundum (Al_2O_3) and/or periclase (MgO), from phase transitions or decomposition during ultrasonic measurements.

at the entire P–T conditions show that the specimen remains in pure spinel phase and there is no other phases observed from phase transitions or decomposition throughout our ultrasonic measurements, as compared to the phase relations in $MgAl_2O_4$ spinel by Akaogi et al.[21]

On the basis of the travel time and sample length data in Table 1, the elastic wave velocities (V_P and V_S) for $MgAl_2O_4$ spinel are derived and plotted as a function of pressure in Figure 4. Fitting the present sound velocity data to the third-order finite strain equations,[31] we obtained compressional (V_P = 9.746(13) km/s) and shear (V_S = 5.522(5) km/s) wave velocities at ambient conditions, which show excellent agreement with those by Lewis et al.[11] (V_P = 9.76 km/s; V_S = 5.50 km/s) and Askarpour et al.[15] (V_P = 9.82 km/s; V_S = 5.50 km/s), respectively. As shown in Figure 4, the compressional velocity (V_P) exhibits a significant increase from 9.746(13) km/s (extrapolated) to 10.391(2) km/s with pressures increasing from 0 to 12.8 GPa at room temperature. The resultant pressure dependence ($\partial V_P/\partial P \approx 0.046(1)$ km/s·GPa^{-1}) is comparable to $\partial V_P/\partial P \approx 0.047(5)$ km/s·GPa^{-1} from fluorescence sideband measurement by Chopelas[23] but obviously larger than $\partial V_P/\partial P \approx 0.021$ km/s·GPa^{-1} from theoretical calculations by Caracas et al.[22] In contrast, a weak increase in V_S from 5.522(5) to 5.539(2) km/s has been observed for $MgAl_2O_4$ spinel within the same pressure range. The current pressure dependence of V_S, $\partial V_S/\partial P \approx 0.0022(5)$ km/s·GPa^{-1}, appears to be consistent with $\partial V_S/\partial P = 0.001(1)$ km/s·GPa^{-1} by Chopelas[23] using fluorescence sideband measurement but significantly different from the theoretically negative pressure dependence in V_S ($\partial V_S/\partial P = -0.014$ km/s·GPa^{-1}) by Caracas.[22] In addition, the trends in V_P and V_S as a function of pressure from our experimental observations are consistent with those from our first-principles calculations (Figure 4). Interestingly, this low pressure dependence in V_S

dx.doi.org/10.1021/jp404901a | J. Phys. Chem. C 2013, 117, 24518–24526

Table 1. Experimental Ultrasonic and in Situ X-ray Data of $MgAl_2O_4$ Spinel

*P (GPa)	T (K)	ρ (g/cm³)	l (mm)	V_P (km/s)	V_S (km/s)	K_S (GPa)	G (GPa)	P_{-Au} (GPa)
12.8	300	3.797(2)	1.090	10.391	5.539	254.6	116.5	11.9
12.0	300	3.784(5)	1.093	10.380	5.537	253.0	116.0	11.6
11.2	300	3.773(4)	1.094	10.311	5.538	246.8	115.7	10.4
10.2	300	3.757(4)	1.095	10.282	5.540	243.4	115.3	9.7
5.3	300	3.678(1)	1.097	10.050	5.522	222.0	112.2	5.0
13.4	500	3.792(2)	1.090	10.307	5.472	251.5	113.5	12.5
12.8	500	3.782(6)	1.094	10.282	5.481	248.4	113.6	11.8
11.8	500	3.767(4)	1.095	10.243	5.482	244.3	113.2	11.1
11.1	500	3.757(4)	1.096	10.224	5.485	242.0	113.1	10.6
6.0	500	3.674(2)	1.098	9.977	5.461	219.6	109.6	5.7
13.8	700	3.785(2)	1.091	10.244	5.412	249.4	110.9	13.2
13.3	700	3.776(4)	1.093	10.205	5.411	245.9	110.6	12.5
12.2	700	3.760(3)	1.094	10.172	5.410	242.3	110.1	11.8
11.7	700	3.752(6)	1.095	10.158	5.410	240.7	109.8	11.4
6.7	700	3.670(2)	1.099	9.910	5.398	217.8	106.9	6.0
14.2	900	3.777(3)	1.092	10.191	5.352	248.1	108.2	13.9
13.6	900	3.767(3)	1.093	10.149	5.353	244.1	107.9	13.1
12.6	900	3.752(3)	1.094	10.116	5.354	240.5	107.5	12.4
12.4	900	3.749(5)	1.095	10.101	5.355	239.1	107.5	12.1

*Pressures are calculated using the equation: $P = -3K_{S(0,T)}\cdot\varepsilon(1-2\varepsilon)^{5/2}[1+3(4-K'_{S(0,T)})\varepsilon/2]$. The uncertainties are less than 0.3% in elastic wave shear velocities and less than 1.5% in the derived elastic moduli. The densities at different high $P-T$ conditions are calculated using the present unit-cell volume and the theoretical density (V_0 = 527.22(43) Å³ and ρ = 3.585(3) g/cm³) from our synchrotron X-ray observations. For a good understanding, the pressures derived from the pressure marker (Au) using Anderson's scale (ref 39) are also shown here.

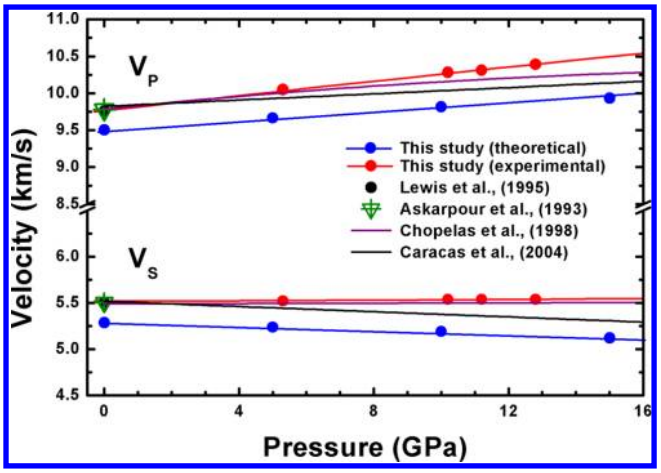

Figure 4. Experimentally observed compressional (V_P) and shear (V_S) wave velocities (red circles) and those from first-principle calculations (blue circles) at high pressure and ambient temperature. Red and blue lines are third-order finite strain fits.

seems common for some nonsilicate/germanate spinel, for instance, a pressure derivative of $\partial V_S/\partial P$ = 0.0007(6) km/s·GPa^{-1} in natural gahnite was reported.[26]

The elastic bulk ($\rho V_P^2 = K_S + 4G/3$) and shear ($G = \rho V_S^2$) moduli are calculated from P and S wave velocities and densities (Table 1). All the data in the entire $P-T$ range are fitted simultaneously to obtain the adiabatic bulk and shear modulus at ambient conditions, as well as their pressure and temperature derivatives using third-order finite strain equations. Upon adiabatic compression, the third-order finite strain equations are expressed as the following[32,40]

$$\rho V_P^2 = (1-2\varepsilon)^{5/2}(L_1 + L_2) \quad (1)$$

$$\rho V_S^2 = (1-2\varepsilon)^{5/2}(M_1 + M_2) \quad (2)$$

$$M_1 = G_{(0,T)} \quad (3)$$

$$M_2 = 5G_{(0,T)} - 3K_{S(0,T)}G'_{(0,T)} \quad (4)$$

$$L_1 = K_{S(0,T)} + \frac{4G_{(0,T)}}{3} \quad (5)$$

$$L_2 = 5L_1 - 3K_{S(0,T)}\left(K'_{S(0,T)} + \frac{4G'_{(0,T)}}{3}\right) \quad (6)$$

$$V_{(0,T)} = V_{(0,300)} \exp \int \alpha dT \quad (7)$$

$$\left(\frac{\partial T}{\partial P}\right)_S = \frac{\gamma T}{K_S} \quad (8)$$

$$M_{(0,T)} = G_0 + (T-300)\left(\frac{\partial M}{\partial T}\right)_P \quad (9)$$

$$M'_{(0,T)} = M'_0 + (T-300)\left(\frac{\partial^2 M}{\partial P \partial T}\right)_P + \left(\frac{\partial M}{\partial T}\right)_P\left(\frac{\gamma T}{K_S}\right) \quad (10)$$

where the subscript (P,T) indicates values at the pressure P and adiabatic foot temperature T, the strain $\varepsilon = [1-(V_{(0,T)}/V)^{2/3}]/2$, in which the volume $V_{(0,T)}$ determined from thermal expansivity $\alpha = 2.14(5)\times10^{-5} + 0.54(4)\times10^{-8}$ T (ref 41.); γ is the Grûneisen parameter constrained by $\gamma\rho$ = constant; M, M', $(\partial M/\partial T)_P$, and $(\partial^2 M/\partial P\partial T)_P$ are the adiabatic bulk (K_S) and shear modulus (G), and their pressure derivatives ($K'_S$and G'), temperature derivatives ($(\partial K_S/\partial T)_P$ and $(\partial G/\partial T)_P$), and cross derivatives ($(\partial^2 K_S/\partial P\partial T)_P$ and $(\partial^2 G/\partial P\partial T)_P$). All temperatures reached in the entire experiment are assumed to be raised along separate adiabats from different foot temperatures T, which are obtained by the integration of eq 8. The properties at these foot temperatures and zero pressure are

dx.doi.org/10.1021/jp404901a | J. Phys. Chem. C 2013, 117, 24518−24526

indicated by subscript (0,T) and related to their properties at ambient conditions (1 bar, 300 K) by eqs 7, 9, and 10. The fitted coefficients, M_1, M_2, L_1, and L_2, calculated by M and M' at zero pressure and adiabat T using eqs 3−10 are applied to calculate compressional and shear wave velocities (V_P and V_S) from eqs 1 and 2, respectively.

We fit all the velocity and density data (after heating) of the entire $P-T$ range to eqs 1−10 by minimizing the difference between the calculated and the observed compressional and shear velocities. Figure 5 shows the P- and S-wave velocity

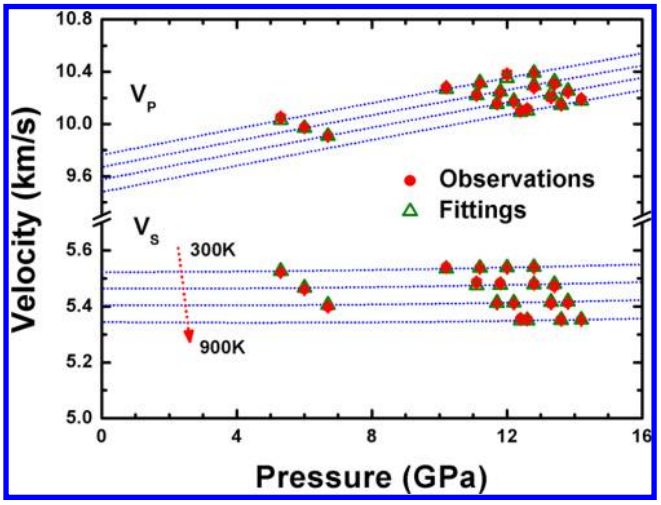

Figure 5. Finite strain fitting (olivine triangle) and observed (red circle) results of compressional (V_P) and shear (V_S) wave velocities of $MgAl_2O_4$ polycrystalline spinel as a function of pressure and temperature. Error bars indicate two standard deviations. Blue dash lines are eye-guide for isotherms.

changes in polycrystalline $MgAl_2O_4$ spinel as a function of pressure and temperature. The compressional wave velocity (V_P) exhibits a systematic increase with pressures and a decrease with temperatures, whereas an almost constant shear wave velocity (V_S) with pressures is observed. This unusual weak pressure dependence in V_S, namely $\partial V_S/\partial P \approx 0.0022(5)$ km/s·GPa^{-1}, is an order of magnitude lower than those for silicate/germanate spinel counterparts[42,43] (e.g., Mg_2SiO_4 spinel,[42] $\partial V_S/\partial P$ = 0.021 kms^{-1}/GPa; Mg_2GeO_4 spinels,[43] $\partial V_S/\partial P$ = 0.015 kms^{-1}/GPa), respectively. Although the low pressure-dependence in shear wave velocity ($\partial V_S/\partial P$ = 0.001(1) km/s·GPa^{-1}) for $MgAl_2O_4$ spinel was proposed by Chopelas[23] using fluorescence sideband measurements, the current data, however, provide a tighter constraint on $\partial V_S/\partial P$ due to the intrinsic high precision of ultrasonic interferometric measurements in comparison with sideband measurements.

Previous theoretical calculations[33,34] indicated that the effect of pressure on cation disorder of $MgAl_2O_4$ was negligible at the present experimental pressure range (0−14 GPa). As shown in Figure 5, along different isotherms both V_P and V_S exhibit pressure dependence similar to those observed at room temperature, suggesting that no order−disorder phase transitions or transformations occurred throughout our experiments.[21] The derived temperature dependence in V_P ($\partial V_P/\partial T \approx -0.00047(2)$ km s^{-1}/K) is in good agreement with that ($\partial V_P/\partial T \approx -0.00040(3)$ km s^{-1}/K) from Brillouin scattering study by Askarpour et al.[15] within mutual uncertainties. In contrast, our result of $\partial V_S/\partial T \approx -0.00032(1)$ km s^{-1}/K is slightly larger than that ($\partial V_S/\partial T \approx -0.00026(2)$ km s^{-1}/K) by Askarpour et al.[15] In comparison with Mg_2SiO_4 spinel, the present temperature dependence in V_P for $MgAl_2O_4$ spinel ($\partial V_P/\partial T \approx -0.00047(2)$ km s^{-1}/K) is significantly smaller than that ($\partial V_P/\partial T \approx -0.00053$ km s^{-1}/K) for Mg_2SiO_4 spinel,[44] whereas our $\partial V_S/\partial T \approx -0.00032(1)$ km s^{-1}/K is almost the same with the value of $\partial V_S/\partial T \approx -0.00031$ km s^{-1}/K for Mg_2SiO_4 spinel.[44]

In view of the $P-T$ range in this study, the cross derivatives of $(\partial^2 K_S/\partial P\partial T)_P$ and $(\partial^2 G/\partial P\partial T)_P$ are assumed to be zero, so that their effects may be reflected in the derived elastic properties. However, given that $(\partial^2 K_S/\partial P\partial T)_P$ and $(\partial^2 G/\partial P\partial T)_P$ are on the order of $\sim 10^{-4}$ for most minerals, as seen in eq 10, its overall effect on the pressure derivatives within 300−900 K is on the order of 0.06, which is negligible. Fitting to the current data yielded K_{S0} =196.0(9) GPa, G_0 = 109.0(4) GPa, $\partial K_S/\partial P$ = 4.60(9), $\partial G/\partial P$ = 0.58(3), $\partial K_S/\partial T$ = −0.022(3) GPa/K, and $\partial G/\partial T$ = −0.014(1) GPa/K (see Table 2). As shown in Figure 5, the fitting results are well consistent with the observed velocities, and the rms velocity misfit is ∼0.013 km/s for V_P and ∼0.005 km/s for V_S, respectively. Figure 6 shows that the bulk modulus increases systematically with pressure and decreases with temperature. Note that the current pressure dependence of the shear modulus, $\partial G/\partial P$ = 0.58(3), is significantly smaller than those for silicate/germanate spinel

Table 2. Comparison of Elastic Properties of Spinel Structured Materials

compound	K_{S0} (GPa)	G_0 (GPa)	$(\partial Ks/\partial P)_T$	$(\partial G/\partial P)_T$	$(\partial K_S/\partial T)_P$ (GPa/K)	$(\partial G/\partial T)_P$ (GPa/K)	ref.
$MgAl_2O_4$	196.0(9)	109.0(4)	4.60(9)	0.58(3)	−0.022(3)	−0.014(1)	this study
	200	109			−0.019(1)	−0.012(1)	Askarpour et al.[a]
	210.1	108.3			−0.015	−0.012	Cynn et al.[b]
	198	109	5.7	0.4(5)			Yoneda[c]
	198(1)	109(1)	5.1(1)	0.07(1)			Chopelas et al.[d]
	196(1)		4.7(3)				Kruger et al.[e]
$(Zn_{0.74}Fe_{0.18}Mg_{0.08})Al_{1.99}O_4$	209(5)	104(3)	4.8(3)	0.5(2)			Reichmann et al[f]
Fe_3O_4 (magnetite)	186(3)	60(3)	5.1(1)	−0.1(1)			Reichmann et al[g]
$(Mg_{0.91}Fe_{0.09})_2SiO_4$	186(1)	119(1)	4.3(1)	1.2(1)	−0.018(1)	−0.015(1)	Higo et al.[h]
Mg_2SiO_4	185(2)	120(1)	4.5(2)	1.5(1)			Li[i]
Mg_2GeO_4	168	104	4.1(2)	1.2(1)			Rigden et al.[j]

[a]Brillouin scattering spectroscopy (ref 15). [b]Ultrasonic resonance (ref 12). [c]Ultrasonic measurements (ref 13). [d]Fluorescence sideband measurements (ref 23). [e]Isothermal values from Static compression (ref 17). [f]Ultrasonic measurements (ref 26). [g]Ultrasonic interferometry (ref 27). [h]Ultrasonic interferometry (ref 45). [i]Ultrasonic interferometry (ref 42). [j]Ultrasonic interferometry (ref 43).

dx.doi.org/10.1021/jp404901a | J. Phys. Chem. C 2013, 117, 24518−24526

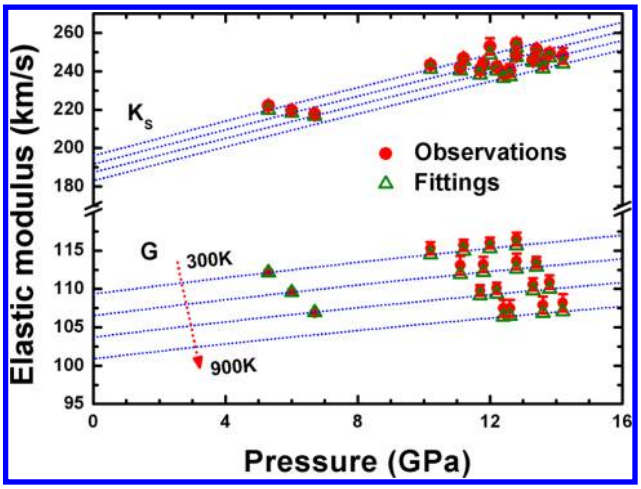

Figure 6. Finite strain fitting (olivine triangle) and measured (red circle) results of bulk (K_S) and shear (G) moduli of $MgAl_2O_4$ polycrystalline spinel as a function of pressure and temperature. Error bars indicate two standard deviations. Blue dash lines are eye-guide for isotherms.

(see Table 2; Mg_2SiO_4 spinel,[42] $\partial G/\partial P$ = 1.5(1); Mg_2GeO_4 spinel,[43] $\partial G/\partial P$ = 1.2(1)).

The present temperature dependence in bulk modulus ($\partial K_S/\partial T$ = −0.022(3) GPa/K) agrees well within the mutual uncertainties with $(\partial K_S/\partial T)_P$ = −0.019(1) GPa/K for $MgAl_2O_4$ spinel by Askarpour et al.[15] using Brillouin scattering spectroscopy, but is slightly larger than the value $(\partial K_S/\partial T)_P$ = −0.015 GPa/K for natural spinel specimen by Cynn et al.[12] (Table 2). For the shear modulus, our result $(\partial G/\partial T)_P$ = −0.014(1) GPa/K agrees with $(\partial G/\partial T)_P$ = −0.012 GPa/K reported by Cynn et al.,[12] and shows almost the same value as that ($(\partial G/\partial T)_P$ = −0.015(1) GPa/K) for $(Mg_{0.91}Fe_{0.09})_2SiO_4$ silicate spinel.[39]

The pressure dependence of bulk modulus for $MgAl_2O_4$ spinel $(\partial K_S/\partial P)_T$ = 4.60(9) is in good agreement with $(\partial K_T/\partial P)_T$ = 4.7(3) from static compression experiments,[17] but smaller than those of $(\partial K_S/\partial P)_T$ = 5.7(3) and 5.1 from previous studies,[13,23] respectively. We attribute these differences to the limited pressure range (~6.2 GPa) and/or inaccurate pressure calibration (i.e., a calibration curve fitted by some fixed points),[13] as well as the vibrational mode dependent velocity/modulus.[23] When comparing with nonsilicate/germanate spinels, our $(\partial K_S/\partial P)_T$ is consistent with that ($(\partial K_S/\partial P)_T$ = 4.8(3)) for natural $(Zn_{0.74}Fe_{0.18}Mg_{0.08})Al_{1.99}O_4$ gahnite spinel[26] within their mutual uncertainties, but smaller than that ($(\partial K_S/\partial P)_T$ = 5.1(1)) for Fe_3O_4 magnetite spinel.[27] Moreover, our $(\partial K_S/\partial P)_T$ is nearly identical to that ($(\partial K_S/\partial P)_T$ = 4.5(2)) for Mg_2SiO_4 silicate spinel,[42] but larger than that for Mg_2GeO_4 germanate spinel ($(\partial K_S/\partial P)_T$ = 4.1(2))[43] (Table 2).

As shown in Figure 6 and Table 2, a weaker pressure dependence in shear modulus ($\partial G/\partial P$ = 0.58(3)) for $MgAl_2O_4$ spinel was observed. This unusual behavior was previously proposed by Yoneda[13] using off-line ultrasonic measurements at room temperature ($\partial G/\partial P$ = 0.4(5)), and by Chopelas[23] using fluorescence sideband technique ($\partial G/\partial P$ = 0.07(1)).[23] However, the large uncertainty[13] in $\partial G/\partial P$, as well as the strongly vibrational mode-dependent results[23] raised doubts about the possible weak pressure dependence in shear modulus. It is interesting to find that this weak pressure dependence in shear modulus seems common for nonsilicate/germanate spinels, such as natural $(Zn_{0.74}Fe_{0.18}Mg_{0.08})Al_{1.99}O_4$ gahnite[26] ($\partial G/\partial P$ = 0.5(2)) and Fe_3O_4 magnetite[27] ($\partial G/\partial P$ = −0.1(1)). It should be noted here that the negative pressure dependence of the shear modulus for Fe_3O_4 magnetite was proposed to be owing to the magnetism effect by 3d transition-metal Fe.[27] Our first-principles calculations show that, for $MgAl_2O_4$ spinel, the tetragonal shear modulus $C_S = (C_{11}-C_{12})/2$ decreases with pressure, which further supports our observed experimental results. We thus concluded that it is the acoustic mode softening, as compared with silicate/germanate spinels (Table 2), that is responsible for the unusual pressure effect on the shear modulus (i.e., a weak pressure dependence in shear modulus of $\partial G/\partial P$ = 0.58(3)) in $MgAl_2O_4$ spinel .

When comparing with MgO_6 octahedra in Mg_2SiO_4 spinel,[46] our first-principles calculations of AlO_6 octahedra in $MgAl_2O_4$ spinel show smaller compressibility. In contrast, the MgO_4 tetrahedra in $MgAl_2O_4$ spinel are more compressible than SiO_4 tetrahedra in Mg_2SiO_4 spinel (Figure 7). As suggested by Recio

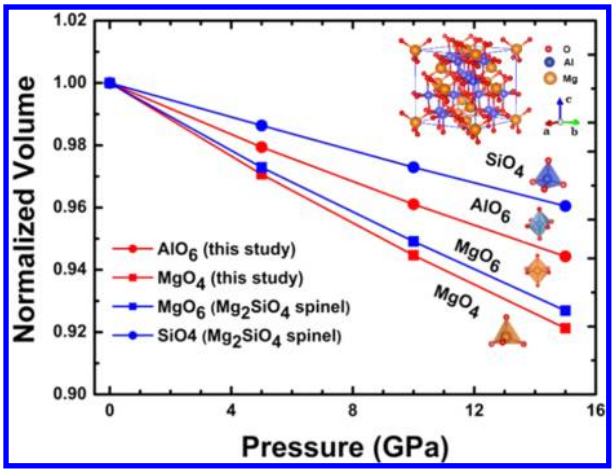

Figure 7. Compressibility of the coordinated polyhedra of $MgAl_2O_4$ spinel and Mg_2SiO_4 ringwoodite.

et al,[47] the weighed average of polyhedral moduli should contribute to the macroscopic bulk properties. The previous study on polyhedral modeling of Mg_2SiO_4 mineral properties by Hazen (ref 48) suggested that silicate tetrahedral (SiO_4) displayed little variation in compression, even with structural transformations induced by pressure and/or temperature. In $MgAl_2O_4$ spinel, the average Al−O distances ranging from 1.9 to ~2.0 Å (octahedral volume changes ~5%), are much larger than those for SiO_4 tetrahedra (volume changes ~2.4%). Similarly, the intraoctahedral O−Al−O angles may deviate by about 15° (about 17%) from the ideal value 90°, which is much larger than those for O−Si−O intratetrahedral angles (no more than 9%).

Our first principles calculations show that the intraoctahedral O−Al−O bond angels change from 82.84 to 83.21° (~0.37°) with pressures ranging from 0 to 15 GPa, whereas the O−Mg−O octahedral angles almost exhibit the same value of 109.47°. Therefore, based on our theoretical calculations and Hazen's study,[49] it appears that AlO_6 octahedra are more easily to be distorted in geometry than SiO_4 (and MgO_4) tetrahedral, but less flexible than MgO_6 octahedra, where the O−Mg−O bond angles sometimes deviated by more than 20° from the ideal octahedral value 90°. Therefore, unusual weak pressure dependence in shear properties may be observed when the

dx.doi.org/10.1021/jp404901a | J. Phys. Chem. C 2013, 117, 24518−24526

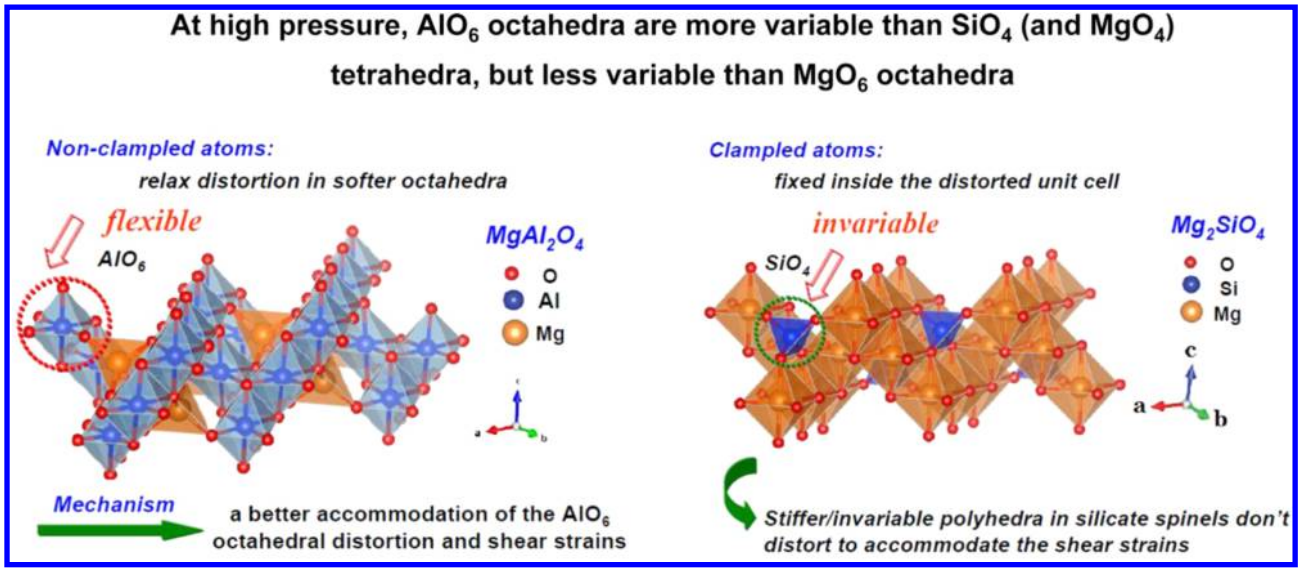

Figure 8. A possible mechanism for the unusual pressure effect on the shear modulus in $MgAl_2O_4$ spinel.

strains are accommodated by flexible polyhedral tilting/distortion and/or symmetry changes.

The mechanism for the shear mode softening or the unusual weak behavior on the shear modulus with pressures can also be explained by two kinds of atoms (i.e., clamped atoms/fixed and nonclamped/flexible atoms) that are defined based on the study by Caracas et al.[22] (Figure 8). At high pressure, the atoms (i.e., clamped atoms) are fixed inside the distorted unit cell, so the coordinated polyhedra do not distort to accommodate the strain; this will result in a strong pressure-dependence in elastic constants. For instance, C_{11} changes from 273.1 at 0 GPa to 322.2 at 15 GPa by our first-principles calculations, yielding $\partial C_{11}/\partial P \approx 3.3$. For nonclamped/flexible atoms, the atoms are allowed to relax at high pressure and thus the octahedral distortion is adjusted to better accommodate the shear strains. Therefore, the pressure-induced tilting/distortion and/or symmetry changes in $MgAl_2O_4$ spinel may result in its weak pressure dependence in shear modulus.

Moreover, it is widely accepted that the slip direction in Mg−Al spinel is always observed to be parallel to the ⟨110⟩ close-packed direction of the face-centered cubic (fcc) lattice.[8] Our theoretical calculations show that the tetragonal shear modulus $C_S = (C_{11}-C_{12})/2$ decreases with pressures, indicating at high pressure the acoustic mode softens for the shear velocity associated with ⟨110⟩ slip direction. From the viewpoints of elastic shear constants, the resultant negative pressure dependence in C_S as well as a small $\partial C_{44}/\partial P = 0.68$ should be responsible for the weak $\partial G/\partial P$ in Mg−Al spinel.

The acoustic modes of lattice vibration are related to the compressional (V_P) and shear (V_S) wave velocities, respectively. The acoustic Debye temperature Θ is described as $\Theta = (h/k)(3N/4\pi)^{1/3}(\rho/(M/Z))^{1/3}(1/(3V_P^3)) + (2/(3V_S^3))^{(-1/3)}$,where M is the molecular mass; Z is the number of atoms in the molecular formula; and k, h, and N are Boltzmann's constant, Planck's constant, and Avogadro's number, respectively. Using the obtained elastic wave velocities and the density data at ambient condition ($V_P = 9.746(13)$ km/s, $V_S = 5.522(5)$ km/s, $\rho = 3.585(3)$ g/cm^3), the Debye temperature Θ_0 is determined to be 866 K, which is in good agreement with the value of Θ_0 = 880 K reported by Catti et al.[50] from Anderson's approximation.[51]

In order to gain further insights into the intricate relation between hardness and elastic moduli, an empirical hardness model,[52] $H_V = 2(k^2G) - 3$(GPa), is introduced, in which k is the Pugh's modulus ratio $k = G/K_S$. Using this model, the Vickers hardness is determined to be 12.9 GPa on the basis of the present derived data, well consistent with the experimental hardness H_V =12.6 GPa.[53] Supposing this model suitable for materials at high pressure, the increasing bulk modulus and a nearly constant shear modulus may be yielding a lower hardness value with increasing pressure (Figure 6). Chen et al.[52] proposed that the modulus ratio k is regarded as an indicator of the brittleness or ductility of materials. The higher k is, the more brittle (and less ductile) the material is. It is thus considered that $MgAl_2O_4$ spinel may become more ductile at high pressure.

IV. CONCLUSIONS

Acoustic velocities and elastic properties of $MgAl_2O_4$ spinel have been measured at simultaneous high pressure and high temperature using ultrasonic interferometry in conjunction with X-ray diffraction. In this study, we report a possible mechanism for the unusual pressure effect on the shear modulus, and the ambient condition adiabatic bulk and shear moduli as well as their pressure and temperature derivatives using a finite strain equation approach. It is worth noting that the present fitting procedure using finite strain equations is independent of the pressure. Therefore, the accuracy of the equation of state of the pressure marker has no effect on the derived thermoelastic properties. Compressional wave velocity (V_P) for $MgAl_2O_4$ spinel increases systematically with pressure and decreases with temperature, which is in contrast to an almost constant shear wave velocity (V_S) with increasing pressure. In this study, we observed a weak pressure dependence in shear modulus for $MgAl_2O_4$ spinel in shear modulus (i.e., the unusual pressure effect on the shear modulus, $\partial G/\partial P = 0.58(3)$), which is significantly smaller than those for silicate/germanate spinel (Mg_2SiO_4 spinel,[42] $\partial G/\partial P = 1.5(1)$; Mg_2GeO_4 spinel,[43] $\partial G/\partial P = 1.2(1)$). Our first-principles calculations shows that the tetragonal shear modulus $C_S = (C_{11}-C_{12})/2$ decreases with pressures, indicating acoustic mode softening, which further supports our experimentally observed unusual elastic behavior

dx.doi.org/10.1021/jp404901a | J. Phys. Chem. C 2013, 117, 24518−24526

in shear modulus at high pressure. In addition, gradual changes in both V_P and V_S versus pressure and temperature suggest that no order−disorder phase transitions/transformations happened up to 14 GPa and 900 K.[21] At high pressure, the coupling between atomic displacements and shear strains can explain the unusual pressure effect on the shear modulus, namely the tilting/distortion and/or symmetry changes in $MgAl_2O_4$ spinel.

AUTHOR INFORMATION

Corresponding Author

*E-mail: yongtao.zou@stonybrook.edu. Tel.: +1-631-632-8338. Fax: +1-631-632-8140.

Notes

The authors declare no competing financial interest.

ACKNOWLEDGMENTS

Y.Z. thanks Robert C. Liebermann for giving fruitful suggestions and Chunyin Zhou for the assistance at Spring-8. The authors also appreciate Y. Kono, Xuefei Li, Xuebing Wang, Ting Chen, and David Welch for their inspiring discussions. This research is supported by the Grant-in-Aid for Young scientist from the Japanese government to S.G. (Proposal No. 23740339) and also supported by the Global-COE program "Deep Earth Mineralogy" to T.I., as well as partially supported by NSF (EAR1045630) and DOE/NNSA (DEFG5209NA 29456) to B.L.

REFERENCES

(1) Ghosh, A.; White, K. W.; Jenkins, M. G.; Kobayashi, A. S.; Brad, R. C. Fracture Resistance of a Transparent Magnesium Aluminate Spinel. *J. Am. Ceram. Soc.* **1991**, *74*, 1624−1630.

(2) Gusmano, G.; Montesperelli, G.; Nunziante, P.; Traversa, E. Microstructure and Electrical Properties of $MgA1_2O_4$ and $MgFe_2O_4$ Spinel Porous Compacts for Use in Humidity Sensors. *Br. Ceram. Trans.* **1993**, *92*, 104−108.

(3) Zou, Y.; He, D.; Wei, X.; Yu, R.; Lu, T.; Chang, X.; Wang, S.; Lei, L. Nanosintering Mechanism of $MgAl_2O_4$ Transparent Ceramics under High Pressure. *Mater. Chem. Phys.* **2010**, *123*, 529−533.

(4) Zou, Y. Precise Determination of the Elasticity and Sound Velocities of Polycrystalline $Mg_3Al_2(SiO_4)_3$ Garnet and $MgAl_2O_4$ Spinel at High Pressure and High Temperature Using Ultrasonic Interferometry In Conjunction With In Situ X-ray Measurements in Multi-anvil Apparatus. Ph.D Thesis, Ehime University: Japan, 2012.

(5) Smith, R.; Bacorisen, D.; Uberuaga, B. P.; Sickafus, K. E.; Ball, J. A.; Grimes, R. W. Dynamical Simulations of Radiation Damage in Magnesium Aluminate Spinel, $MgAl_2O_4$. *J. Phys.: Condens. Matter* **2005**, *17*, 875−891.

(6) Li, J. G.; Ikegami, T.; Lee, J. H.; Mori, T.; Yajima, Y. Synthesis of Mg-Al Spinel Powder via Precipitation Using Ammonium Bicarbonate as the Precipitant. *J. Eur. Ceram. Soc.* **2001**, *21*, 139−148.

(7) Patterson, M. C. L.; Caiazza, J. E.; Roy, D. W. Transparent Spinel Development. *Proc. SPIE.* **2000**, *4102*, 59−68.

(8) Mitchell, T. E. Dislocations and Mechanical Properties of MgO-Al_2O_3 Spinel Single Crystals. *J. Am. Ceram. Soc.* **1999**, *82*, 3305−3316.

(9) Irifune, T.; Fujino, K.; Ohtani, E. A New High-pressure Form of $MgAl_2O_4$. *Nature* **1991**, *349*, 409−411.

(10) Irifune, T.; Naka, H.; Sanehira, T.; Toru, T.; Funakoshi, K. In Situ X-ray Observations of Phase Transitions in $MgAl_2O_4$ Spinel to 40 GPa Using Multianvil Apparatus with Sintered Diamond Anvils. *Phys. Chem. Miner.* **2002**, *29*, 645−654.

(11) Lewis, M. F. Elastic Constants of Magnesium Aluminate Spinel. *J. Acoust. Soc. Am.* **1966**, *40*, 728−729.

(12) Cynn, H.; Anderson, O. L.; Nicol, M. Effects of Cation Disordering in A Natural $MgAl_2O_4$ Spinel Observed by Rectangular Parallelepiped Ultrasonic Resonance and Raman Measurements. *Pure Appl. Geophys.* **1993**, *141*, 415−444.

(13) Yoneda, A. Pressure Derivatives of Elastic Constants of Single Crystal MgO and $MgAl_2O_4$. *J. Phys. Earth* **1990**, *38*, 19−55.

(14) Chang, Z. P.; Barsch, G. R. Pressure Dependence of Single-Crystal Elastic Constants and Anharmonic Properties of Spinel. *J. Geophys. Res.* **1973**, *78*, 2418−2433.

(15) Askarpour, V.; Manghnani, M. H.; Fassbender, S.; Yoneda, A. Elasticity of Single-Crystal $MgAl_2O_4$ Spinel up to 1273 K by Brillouin Spectroscopy. *Phys. Chem. Miner.* **1993**, *19*, 511−519.

(16) Suzuki, I.; Ohno, I.; Anderson, O. L. Harmonic and Anharmonic Properties of Spinel $MgAl_2O_4$. *Am. Mineral.* **2000**, *85*, 304−311.

(17) Kruger, M. B.; Nguyen, J. H.; Caldwell, W.; Jeanloz, R. Equation of State of $MgAl_2O_4$ Spinel to 65 GPa. *Phys. Rev. B* **1997**, *56*, 1−4.

(18) Levy, D.; Pavese, A.; Hanfland, M. Synthetic $MgAl_2O_4$ (Spinel) at High-Pressure Conditions (0.0001−30 GPa): A Synchrotron X-Ray Powder Diffraction Study. *Am. Mineral.* **2003**, *88*, 93−98.

(19) Gracia, L.; Beltran, A.; Andres, J.; Franco, R.; Recio, J. M. Quantum-mechanical Simulation of $MgAl_2O_4$ under High Pressure. *Phys. Rev. B* **2002**, *66*, 224114(1)−224114(7).

(20) Ono, S.; Brodholt, J. P.; Price, G. D. First-Principles Simulation of High-Pressure Polymorphs in $MgAl_2O_4$. *Phys. Chem. Miner.* **2008**, *35*, 381−386.

(21) Akaogi, M.; Hamada, Y.; Suzuki, T.; Kobayashi, M.; Okada, M. High Pressure Transitions in the System $MgAl_2O_4$-$CaAl_2O_4$: A New Hexagonal Aluminous Phase with Implication for the Lower Mantle. *Phys. Earth Planet. Inter.* **1999**, *115*, 67−77.

(22) Caracas, R.; Banigan, E. J. Elasticity and Raman and Infrared Spectra of $MgAl_2O_4$ Spinel from Density Functional Perturbation Theory. *Phys. Earth Planet. Inter.* **2009**, *174*, 113−121.

(23) Chopelas, A. The Fluorescence Sideband Method for Obtaining Acoustic Velocities at High Compressions: Application to MgO and $MgAl_2O_4$. *Phys. Chem. Miner.* **1996**, *23*, 25−37.

(24) Kung, J.; Li, B.; Uchida, T.; Wang, Y.; Neuville, D.; Liebermann, R. C. In Situ Measurements of Sound Velocities and Densities across the Orthopyroxene→High-Pressure Clinopyroxene Transition in $MgSiO_3$ at High Pressure. *Phys. Earth Planet. Inter.* **2004**, *147*, 27−44.

(25) Yeganeh-Haeri, A.; Weidner, D. J. Single Crystal Elasitc Property of $MgAl_2O_4$ up to 1200 K. *EOS Trans., Am. Geophys. Union* **1990**, *71*, 620.

(26) Reichmann, H. J.; Jacobsen, S. D. Sound Velocities and Elastic Constants of $ZnAl_2O_4$ Spinel and Implications for Spinel-elasticity Systematics. *Am. Mineral.* **2006**, *91*, 1049−1054.

(27) Reichmann, H. J.; Jacobsen, S. D. High-pressure Elasticity of a Natural Magnetite Crystal. *Am. Mineral.* **2004**, *89*, 1061−1066.

(28) Liu, W.; Li, B.; Wang, L.; Zhang, J.; Zhao, Y. Elasticity of ω-Phase Zirconium. *Phys. Rev. B* **2007**, *76*, 144107(1)−144107(4).

(29) Zou, Y.; Irifune, T.; Gréaux, S.; Whitaker, M.; Shinmei, T.; Ohfuji, H.; Negishi, R.; Higo, Y. Elasticity and Sound Velocities of Polycrystalline $Mg_3Al_2(SiO_4)_3$ Garnet up to 20 GPa and 1700 K. *J. Appl. Phys.* **2012**, *112*, 14910(1)−14910(9).

(30) Irifune, T.; Higo, Y.; Inoue, T.; Kono, Y.; Ohfuji, H.; Funakoshi, K. Sound Velocities of Majorite Garnet and the Composition of the Mantle Transition Region. *Nature (London)* **2008**, *451*, 814−817.

(31) Liu, W.; Li, B.; Wang, L.; Zhang, J.; Zhao, Y. Simultaneous Ultrasonic and Synchrotron X-ray Studies on Pressure Induced α-ω Phase Transition in Zirconium. *J. Appl. Phys.* **2008**, *104*, 76102(1)−76102(3).

(32) Liu, W.; Kung, J.; Li, B.; Nishiyama, N.; Wang, Y. Elasticity of $(Mg_{0.87}Fe_{0.13})_2SiO_4$ Wadsleyite to 12 GPa and 1073 K. *Phys. Earth Planet. Inter.* **2009**, *174*, 98−104.

(33) Li, L.; Carrez, P.; Weidner, D. Effect of Cation Ordering and Pressure on Spinel Elasticity by *Ab Initio* Simulation. *Am. Mineral.* **2007**, *92*, 174−178.

(34) Hazen, R. M.; Navrotsky, A. Effects of Pressure on Order-Disorder Reactions. *Am. Mineral.* **1996**, *81*, 1021−1035.

(35) Maekawa, H.; Sato, S.; Kawamura, K.; Yokokawa, T. Cation Mixing in Natural $MgAl_2O_4$ Spinel: A High-Temperature 27Al NMR Study. *Am. Mineral.* **1997**, *82*, 1125−1132.

(36) Segall, M.; Lindan, P. J. D.; Probert, M. J.; Pickard, C. J.; Hasnip, P. J.; Clark, S. J.; Payne, M. C. First-Principles Simulation: Ideas,

Illustrations and the CASTEP Code. *J. Phys.: Condens. Matter* **2002**, *14*, 2717−2744.
(37) Vanderbilt, D. Soft Self-Consistent Pseudopotentials in a Generalized Eigenvalue Formalism. *Phys. Rev. B* **1990**, *41*, 7892−7895.
(38) Monkhorst, H. J.; Pack, J. D. Special Points for Brillouin-Zone Integrations. *Phys. Rev. B* **1976**, *13*, 5188−5192.
(39) Anderson, O. L.; Issak, D. G.; Yamamoto, S. Anharmonicity and the Equation of State for Gold. *J. Appl. Phys.* **1989**, *65*, 1534−1543.
(40) Davies, G. F.; Dziewonski, A. M. Homogeneity and Constitution of the Earth's Lower Mantle and Outer Core. *Phys. Earth Planet. Inter.* **1975**, *10*, 336−343.
(41) Fiquet, G.; Richet, P.; Montagnac, G. High-Temperature Thermal Expansion of Lime, Periclase, Corundum and Spinel. *Phys. Chem. Miner.* **1999**, *27*, 103−111.
(42) Li, B. Compressional and Shear Wave Velocities of Ringwoodite (Mg_2SiO_4) to 12 GPa. *Am. Mineral.* **2003**, *88*, 1312−1317.
(43) Rigden, S. M.; Jackson, I.; Niesler, H.; Ringwood, A. E.; Liebermann, R. C. Pressure Dependence of the Eastic Wave Velocities for Mg_2GeO_4 Spinel to 3 GPa. *J. Geophys. Res.* **1988**, *15*, 605−608.
(44) Jackson, J. M.; Sinogeikin, S. V.; Bass, J. D. Sound Velocities and Elastic Properties of γ-Mg_2SiO_4 to 873 K by Brillouin Spectroscopy. *Am. Mineral.* **2000**, *85*, 296−303.
(45) Higo, Y.; Inoue, T.; Irifune, T.; Funakoshi, K.; Li, B. Elastic Wave Velocities of $(Mg_{0.91}Fe_{0.09})_2SiO_4$ Ringwoodite under P−T Conditions of the Mantle Transition Region. *Phys. Earth Planet. Inter.* **2008**, *166*, 167−174.
(46) Kiefer, B.; Stixrude, L.; Wentzcovitch, R. Normal and Inverse Ringwoodite at High Pressures. *Am. Mineral.* **1999**, *84*, 288−293.
(47) Recio, J. M.; Franco, R.; Pendás, A. M.; Blanco, M. A.; Pueyo, L.; Pandey, R. Theoretical Explanation of the Uniform Compressibility Behavior Observed in Oxide Spinels. *Phys. Rev. B* **2001**, *63*, 184101(1)−184101(7).
(48) Hazen, R. M. A Useful Fiction: Polyhedral Modeling of Mineral Properties. *Am. J. Sci.* **1988**, *288-A*, 242−269.
(49) Suzuki, I.; Kumazawa, M. Anomalous Thermal Expansion in Spinel $MgAl_2O_4$. *Phys. Chem. Miner.* **1980**, *5*, 279−284.
(50) Catti, M.; Valerio, G.; Dovesi, R.; Causà, M. Quantum-Mechanical Calculation of the Solid-state Equilibrium MgO+α-Al_2O_3⇄$MgAl_2O_4$ (Spinel) versus Pressure. *Phys. Rev. B* **1994**, *49*, 14179−14187.
(51) Anderson, O. L. A Simplified Method for Calculating the Debye Temperature from Elastic Constants. *J. Phys. Chem. Solids.* **1963**, *24*, 909−917.
(52) Chen, X.-Q.; Niu, H.; Franchini, C.; Li, D.; Li, Y. Hardness of T-Carbon: Density Functional Theory Calculations. *Phys. Rev. B* **2011**, *84*, 121405(1)−121405(5).
(53) Krell, A.; Bales, A. Grain Size-Dependent Hardness of Transparent Magnesium Aluminate Spinel. *Int. J. Appl. Ceram. Technol.* **2011**, *8*, 1108−1114.